A ROBUST SYSTEM FOR SENSING ACOUSTIC EMISSIONS FOR WEARABLE KNEE HEALTH ASSESSEMENT

A Dissertation
Presented to
The Academic Faculty

by

Caitlin Teague

In Partial Fulfillment
of the Requirements for the
Master's Degree in the
School of Electrical and Computer Engineering

Georgia Institute of Technology
December 2016

A ROBUST SYSTEM FOR SENSING ACOUSTIC EMISSIONS FOR WEARABLE KNEE HEALTH ASSESSEMENT

Approved by:

Dr. Omer T. Inan, Advisor
School of Electrical and Computer Engineering
Georgia Institute of Technology

Dr. Farrokh Ayazi
School of Electrical and Computer Engineering
Georgia Institute of Technology

Dr. Géza F. Kogler
School of Biological Sciences
Georgia Institute of Technology

Date Approved: December 7, 2016

ACKNOWLEDGEMENTS

First, I would like to express my sincerest thanks to my advisor, Dr. Omer T. Inan. His extensive knowledge of engineering and physiology, insightfulness during conversations, passion for novel research, and mentorship have been a great source of inspiration.

Additionally, I would like to acknowledge Dr. Farrokh Ayazi and Dr. Géza F. Kogler for their time and consideration as members of my thesis committee.

I would like to acknowledge Sinan Hersek and Hakan Töreyin with whom I worked closely to develop hardware and data processing algorithms for measuring and interpreting joint sounds as well as Jordan L. Conant with whom I worked to implement the wearable prototype. I was privileged to work with such hardworking, creative, and positive teammates. Additionally, I would like to acknowledge Scott M. Gilliland. His prototyping skills and hardware as well as his coding expertise were crucial to completing the wearable system.

To the members of the Inan Research Lab—especially Oludotun Ode, Andrew M. Carek, Nicholas B. Bolus, Jordan L. Conant, Sinan Hersek, and Hazar Ashouri—your help, support, and friendship have been invaluable to my experience as a graduate student.

Lastly, I would like to thank my family who has provided continuous and unconditional love, support, and encouragement.

TABLE OF CONTENTS

LIST OF TABLES

LIST OF FIGURES

extracted from two IMUs placed at the lateral side of the thigh and shank. The sounds were recorded during an unloaded flexion / extension task.

SUMMARY

The objective of the research was to pursue hardware and software that enables wearable measurement of knee joint sounds, ultimately providing a platform to continuously quantify the health of a knee during rehabilitation of an acute injury. This work focuses on the robust *measurement* of joint acoustic emissions in the context of activity. Two sensing modalities—"air" and contact microphones—were used to measure joint sounds, for they provide complementary sensing capabilities for detecting acoustic emissions, which present as airborne signals and as skin vibrations. Inertial measurement data is collected simultaneously with joint sounds to provide physiological context, namely joint angle and activity classification information, and observe the consistency of these signals with respect to particular activities. Characterization of these sensors and demonstration of their high-quality and repeatable measurements are presented. Additionally, a preliminary, wearable, embedded system was implemented to collect data to replace in-lab / in-clinic data acquisition systems.

CHAPTER 1. INTRODUCTION

Musculoskeletal injuries, and the accompanying increased risks of re-injury [1], are a major cause of hospitalization for active young adult, adult, and elderly Americans, particularly veterans [2]. Wearable assistive technologies for monitoring joint health can help patients rehabilitating knee injuries perform physical therapy and assess their progress in the comfort of their home [3-5], or collect objective clinical data during unsupervised rehabilitation programs in athletes and soldiers, provided that the devices are unobtrusive and accurate. The use of such sensor systems might provide a new tool to easily obtain digital health signals that quantify rehabilitation progress and may help to reduce health care costs for patients with joint injuries.

Accordingly, many researchers have attempted to evaluate post-operative rehabilitation status using wearable sensors. Glaros *et al*. have presented a concept of a complex multi-modal system with sensors distributed in various locations on the body to assess athlete rehabilitation progress [6]. Atallah *et al*. showed, using an ear-worn activity recognition sensor, that changes in gait during post-operative recovery could be detected from subjects with simulated knee injury [7].

Research has also focused recently on tracking the acoustics of the joints to assess their health. Shrivastava, and Prakash reviewed the use of acoustic emissions for assessing bone condition [8]. Frank *et al*. concluded that the analysis of knee joint sounds could be used for distinguishing normal from abnormal cartilage surfaces, and for classifying disorders of the joint [9]. In 2010, Glaser *et al*. developed vibration and acoustic measurement techniques to correlate to in vivo kinematics in Total Hip

Arthoplasty [10]. The researchers showed useful correlations between the vibration and acoustics measurements – taken using relatively large sensors attached to bench-top electronics and data acquisition modules – and video fluoroscopy images of in vivo kinematics and femoral head sliding. Similarly, Kim *et al*. placed an electronic stethoscope at the knee joint to characterize the acoustical features of interests for knee sounds, and reported significant differences between normal subjects and patients with knee problems [11]. Mascaro *et al*. presented the concept of differentiating between osteoarthritic and healthy knees based on the number of acoustic emissions occurring during flexion and extension [12]. Importantly, the approaches presented in these previous studies were limited to controlled lab settings, as neither the sensors nor the electronics were miniaturized and the sensor packaging / interfacing to the body was not assessed in the context of wearable, ubiquitous measurement. However, the results suggested that joint sounds and vibrations could provide non-invasive metrics of joint healing progress post-operatively.

The ultimate objective of this research is to quantify changes in joint sounds during recovery from musculoskeletal injury and to then use the characteristics of such sounds as a biomarker for quantifying joint rehabilitation progress. This work focuses on the robust measurement of joint acoustic emissions using miniature microphones placed on the knee and interfaced to custom hardware [13]. Two types of microphones were investigated: (1) miniature microphones with a sound port for detecting airborne sounds and (2) piezoelectric film based contact microphones for detecting skin vibrations associated with internal sounds. Additionally, inertial measurements were taken simultaneously with joint sounds to observe the consistency in the acoustic emissions in

the context of particular activities: knee flexion / extension (without load) and multi-joint weighted movement involving knee and hip flexion / extension (i.e. sit-to-stand). The preliminary data demonstrated that high quality joint sound measurements can be obtained with unique and repeatable acoustic signatures in healthy and injured joints. Additionally, the results suggest that combining piezoelectric contact microphones (which detect high quality acoustic emission signals directly from the skin vibrations but can be compromised with loss of skin contact) and electret microphones (which measure lower signal-to-noise ratio airborne sounds from the joint but can even measure such sounds at 5 cm distance from the skin) can provide robust measurements for a future wearable system to assess joint health in patients during rehabilitation at home.

Furthermore, we have developed a novel, wearable sensing system based on miniature piezoelectric contact microphones for measuring the acoustical emissions from the knee during movement [14]. To our knowledge, this is the first instance of a wearable knee sound sensing system. The system consists of two contact microphones, positioned on the medial and lateral sides of the patella, connected to custom, analog pre-amplifier circuits and a microcontroller for digitization and data storage on a secure digital card. In addition to the acoustical sensing, the system includes two integrated inertial measurement sensors including accelerometer and gyroscope modalities to enable joint angle calculations; these sensors, with digital outputs, are connected directly to the same microcontroller. The system provides low noise, accurate joint acoustical emission and angle measurements in a wearable form factor and has several hours of battery life.

CHAPTER 2. BACKGROUND

Each year, approximately 200,000 Americans endure anterior cruciate ligament (ACL) tears and 100,000 reconstructive procedures are conducted to repair the injured knees [15]. During the long rehabilitation process that follows surgery, no direct quantitative metric for evaluating the biomechanical function of the joint is readily available; instead, clinicians rely on evaluation surrounding muscle strength, various functionality tests such a single leg hop tests, and patient confidence in performing various exercises as a benchmark for determining readiness for return-to-sport [16]. Wearable technologies for quantifying the state of rehabilitation, which may also provide feedback to the user regarding which activities or intensities of activities are safe to perform at any given time, could potentially help accelerate the rehabilitation process as well as reduce the risk of re-injury.

2.1 ACL Injuries

The knee is subject to extreme stress due to the multidirectional forces and large loading requirements it must account for even during ambulatory activities [17-20]. The ACL is one of the primary stabilizing ligaments within the knee, primarily limiting anterior tibial translation and controlling internal rotational stability, which if untreated, is extremely disruptive even for those patients not engaged in competitive activities [21]. In general populations, men are more likely to suffer ACL injuries, likely attributed to their increased exposure to physical activity in everyday living and contact sports [22]. However, women athletes are more susceptible to ACL injuries and tearing the ligament

in non-contact situations [23]. Most patients, especially athletes, elect to have reconstructive surgery with the goal of stabilizing the knee [24].

2.2 Metrics for Determining Return-to-Play

There remain many standards for determining successful outcomes post-surgery. However, it is widely accepted that a patient's return-to-play serves as the ultimate determinant of a successful surgery given that it is at the forefront of most patients' and coaches' minds [24-26]. Currently, no metric that directly captures the physiological state of the joint itself is used for determining return-to-play. Moreover, there are no confirmed quantitative tests for determining progression through rehabilitation [27]. Instead, combinations of evaluation of quadriceps and hamstring strength, range of motion, single-hop tests, swelling, stability and balance, confidence in running and pivoting, and overall functionality of the knee are used to determine a patient's readiness for return-to-sport [16]. While 67% of patients return to sport within 12 months of surgery, only 33% return to their pre-surgery level of play [24]. C. Ardern *et al.* cite that psychological readiness has the largest influence on a patient's return, and numerous studies show lack of confidence and fear of re-injury are large reasons for failure to return [28].

2.3 Complications in the Years Following Injury

In addition to the 44% 5-year re-injury rate [29], osteoarthritis is one of the major sources of complications in the years following ACL injuries [30]. The risk for development of osteoarthritis is higher in patients with ACL injuries; moreover, these patients are more likely for onset of osteoarthritis at younger ages [31]. Lohman *et al.* observed that, in female soccer players, 51% compared to 7% of the index and

contralateral knees, respectively, experienced radiographic knee osteoarthritis 12 years post-injury with a mean age of 31 years [32]. Furthermore, Kessler *et al*. showed that patients who had reconstructive surgery were more osteoarthritic but had better joint stability than those patients who decided on non-surgical methods for treating the injury [33]. However, Øiestad *et al*. has suggested such figures are too high and reported instead that the rate for osteoarthritis onset to be 0% – 13%, and 21% – 48% for those with isolated ACL tears and those that incurred additional injuries (e.g., meniscal tear accompanying the ACL tear), respectively [30]. Regardless of the actual incidence rates, this suggests that ACL injuries and their effects are not limited to months following the injury but instead may have significant influence on the patient's quality of life even years later.

2.4 Review of Knee Joint Acoustics

Acoustical emissions have been used as a means to detect failures or damages in materials [34-36]. More broadly than acoustical emissions, doctors have used auscultation overall as a means for detecting abnormal bodily functions, which are then usually verified using imaging equipment, and research has expanded upon this concept. For example, some research has focused on classifying lung sounds [37, 38] while other research has used heart sounds to screen for various diseases, such as those related to abnormal heart valve function [39].

Acoustical emissions, in particular, have been used for in-clinic examination of joint health, namely knee joint health; primarily, research in this field, or the study of vibroarthographic signals (VAG), has largely focused on using these signals to

differentiate between “healthy” and “unhealthy” knees—primarily those afflicted with cartilage-based conditions—using single-visit recordings of the joint sounds [40]. In addition to binary classifications of knees, J. Lee *et al*. have shown that these sounds may even be used to discriminate between different conditions of the joint [41]. To achieve these classifications, researchers have utilized a variety of sensors for capturing joint sounds; Mollan *et al.* used condenser microphones [42] while L. Shark *et al.* used wide-band piezoelectric sensors [43] to record acoustic emissions in both low (<100 Hz) and high frequency (>20 kHz) bands, respectively. Regardless of the specific sensor-type, more broadly, research has leveraged the use of contact microphones (e.g., accelerometers, piezoelectric devices, stethoscopes) to measure joint sounds, though some early work did explore the use of “air” microphones [40]. This is because contact microphones, theoretically, have the potential to measure the most complete signal, for most of the acoustical energy produced by the friction of internal articulating surfaces of the joint results in skin surface vibrations while only a fraction of the energy is transmitted to the air [42, 44].

While these in-clinic, acoustic-based “diagnostic” techniques are a step towards reducing health-care costs when compared to their imaging counterparts, a gap remains for a large sector of knee joint conditions—those that require substantial rehabilitation. Leveraging the biomarkers of joint sounds, wearable technologies may aid in quantifying the state of rehabilitation, potentially providing feedback to the user regarding which activities or intensities of activities are safe to perform at any given time, and could help accelerate the rehabilitation process as well as reduce the risk of re-injury. Moreover, such technologies may provide return-to-play-based metrics. However, these methods are

only practically feasible given an accurate, unobtrusive, and inexpensive device. As such, this work aims to explore the engineering challenges of measuring joint sounds in a wearable form factor.

CHAPTER 3. INSTRUMENTATION

In conjunction with S. Hersek and H. Töreyin, preliminary circuits and systems were developed to record knee joint sounds. Proof-of-concept experiments were performed to determine the efficacy of measuring joint sounds before extensive human subject studies were conducted. Namely, the preliminary experiments were designed to test the sensitivity of the sensors, determine viable locations for the sensors, and understand the general nature of these sounds (e.g., signal level, primary frequency bands, etc.). The block diagram of the overall system used for collecting joint sound data is presented in Figure 1. All data were recorded on a laptop computer for post-test processing.

With the efforts of J. L. Conant and S. M. Gilliland, this in-lab / in-clinic system was implemented on a wearable, embedded platform. Front-end circuits were designed for MEMS and piezoelectric-based contact microphones. Regardless of microphone type—air or contact—the wearable system is capable of sufficient sample rates for simultaneous measurement of joint sounds and inertial data. This work specifically focuses on the microcontroller-based data collection and saving to a microSD card.

3.1 Sensor Selection

The sounds generated by the joints within the body propagate through the fluid-filled internal tissue to the skin, where there is a lossy acoustical interface to the air; because of the high acoustical impedance mismatch between fluid and air, a small portion of the acoustical energy is then transmitted into the air, while the majority of the energy

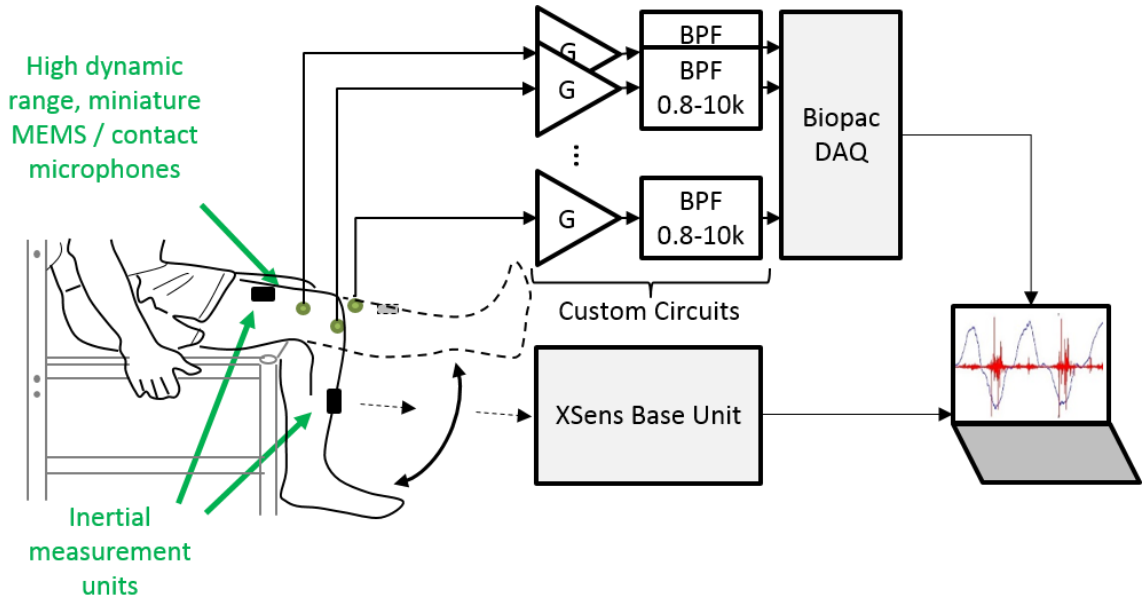

Figure 1. Block diagram of setup used for simultaneous joint sound and inertial measurements. Electret and MEMS microphones are placed laterally and medially to the patella, while piezoelectric film contact microphones were placed proximal and distal to the patella. Signals from the microphones were conditioned via front-end circuits and recorded on a laptop using a Biopac MP150 DAQ. Simultaneously, wireless inertial data was recorded using Xsens hardware and data acquisition software.

is reflected back into the tissue. For this reason, we decided to employ piezoelectric film (SDT, Measurement Specialties, Hampton, VA) based contact microphones on the skin surface to detect the acoustic emissions from the joints. This strategy does not rely on the sounds becoming airborne from the body, and should thus, theoretically, result in the capture of high quality joint sound data. However, in a wearable system with ambulant users performing normal activities of daily living, the microphone-skin interface can be compromised by motion artifacts: in the case of a "contact" measurement, these artifacts may result in the total loss of signal being measured by the sensor. As a result, we have decided to supplement the contact microphones with miniature electret (COS-11D, Sanken Microphones, Tokyo, Japan) and micro-electromechanical systems (MEMS) based microphones (MP33AB01H, ST Microelectronics, Geneva, Switzerland) with a

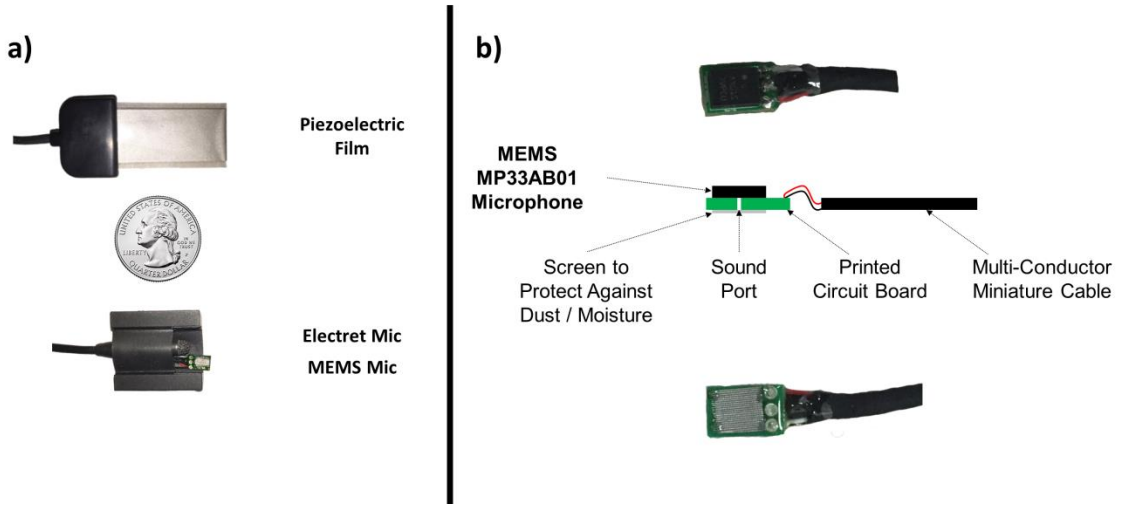

Figure 2. Various microphones used for recording joint sounds. (a) Relative sizes of the piezoelectric film, electret, and MEM-based microphones. (b) Custom MEMS packaging, which includes a custom PCB mount, cabling, and stainless steel mesh for protection of the sound port.

sound port to measure the airborne sounds. These air microphones were specifically chosen for their small size (electret: 16.1 mm x 4.0 mm in length x diameter; MEMS: 3.76 x 2.95 x 1.0 mm in length x width x height), broad bandwidth (electret: 50 – 20,000 Hz; MEMS: 100 – 10,000 Hz), and sensitivity (electret: -35 dB at 1 kHz where 0 dB is 1 V/Pa; MEMS: -38 dBV at 1 kHz where 0 dB is 1 V/Pa). The piezoelectric film was chosen as the contact microphone for its small size and because its form factor seemingly lends itself to a wrap and other devices conventionally worn on the knee.

Although we anticipate that the quality of these airborne sounds will be lower than the contact measurements due to the lossy interface and ambient noise, the manner in which these sounds are compromised during motion will be less catastrophic: unlike contact microphones which require direct physical coupling to sense sound, electret microphones can still sense the joint sounds from centimeters away from the skin surface. The use of both types of microphones in our measurements is novel and will be important

for preserving robustness in the ultimate implementation. A photo of the three sensors used in this work is shown in Figure 2(a).

For the MEMS microphone, custom printed circuit board (PCB) mounting and cabling was developed as shown in Figure 2(b). Special consideration was given towards protecting the sound port of the microphone; accordingly, we attached a stainless steel wire cloth screen (Type 304) to the back of the PCB, covering the sound port to help mitigate microphone sensing degradation due to dust- or other debris-related damage.

3.2 Sensor Interfacing Circuits

We designed custom analog circuits to amplify and filter the signals from the contact and MEMS microphones and then interface these signals to the data acquisition hardware. For the contact microphones, we designed a low-noise, non-inverting amplifier front-end stage with high (10 MΩ) input impedance, gain of 45 dB, and a bandwidth of 800 Hz – 10 kHz; we then used a fourth-order Butterworth Sallen-Key filter with a cutoff frequency of 10 kHz for anti-aliasing and to reduce high frequency noise. For the MEMS microphones, we powered the microphones with a regulated 3.3 VDC supply, and used a low-noise inverting amplifier front-end with adjustable gain, and a bandwidth of 20 Hz – 20 kHz; this stage was also followed by equivalent anti-alias filtering. The microphone signals were sampled at ≥40 kHz using the Biopac (Goleta, CA) data acquisition hardware, and stored on a laptop.

3.3 Proof-of-Concept Experiments

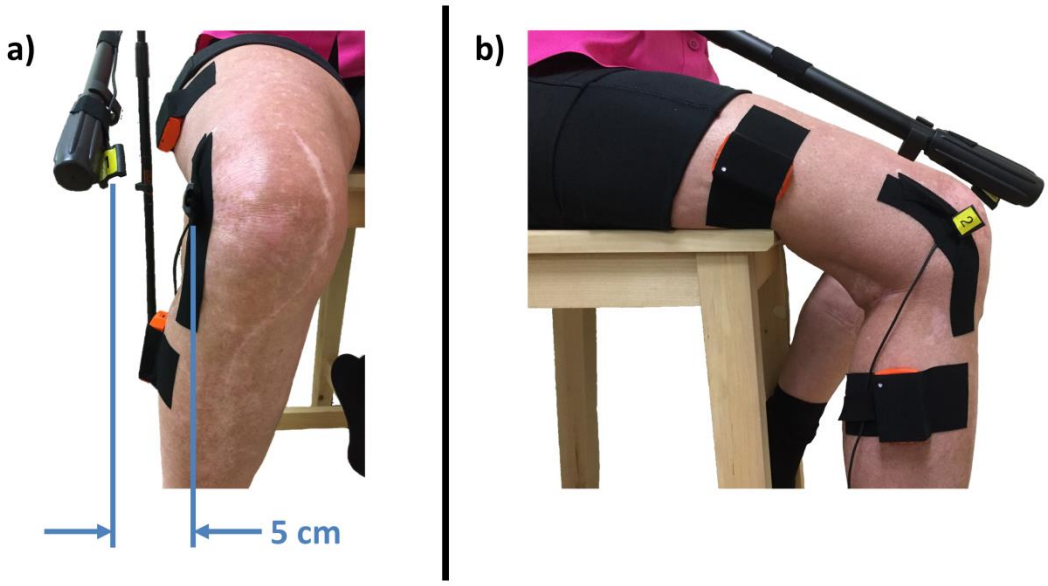

Figure 3. Electret microphone placement for on- vs. off-skin measurements of joint sounds. The microphone is placed lateral of the patella, taped directly on the skin and affixed to a mounting structure 5 cm away. The placements are shown from the sagittal and frontal planes in (a) and (b), respectively.

The studies were approved by the Georgia Institute of Technology Institutional Review Board (IRB) as well as the Army Human Research Protection Office (AHRPO). Four proof-of-concept studies were performed: (1) measuring knee joint sounds during unloaded flexion / extension from one subject to determine the repeatability of the sounds from one flexion / extension cycle to the next; (2) measuring joint sounds during a multi-joint movement involving sit-to-stand from a standardized box height; (3) assessing the feasibility of piezoelectric contact microphones compared to electret microphones for wearable measurements; and (4) measuring joint sounds from a distance of five centimeters off of the surface of the skin with the electret microphones to ensure that airborne sound measurements are feasible even in the absence of direct coupling to the skin.

For the first study, the MEMS microphones were placed directly on the subject's skin on the lateral and medial sides of the patella using Kinesio tape. The determination of microphone placement was based on previous reports [12], and pilot testing within the investigative team to identify optimal recording sites with maximal signal level. The subjects who participated in these proof-of-concept experiments contained individuals across a range of knee joint health status with diagnosed knee osteoarthritis to no previous knee joint injury. For the second proof-of-concept study, the microphones were lifted off of the surface of the skin by five centimeters and held in place by a fixture as the subject performed the same activities as shown in Figure 3. In addition to the microphones described above, we placed two inertial measurement units (IMUs), each with a built-in three-axis accelerometer, gyroscope, and magnetometer, on the quadriceps and the tibia to calculate joint angle (MTW-38A70G20, XSens, Enschede, The Netherlands).

3.4 Joint Sound Processing in the Context of Activity

We developed initial methods to analyze the knee joint acoustic emissions in the context of joint angle using Matlab (The Mathworks, Natick, MA) in post-processing. The approach consists of two main parts: preprocessing the sound data and automatically locating the cycles. The sound data is preprocessed by applying a bandpass filter that limits the signal from 1 to 10 kHz. From our initial recordings, this frequency range seems to include mainly acoustical components associated with the joints, and rejects low frequency ambient noise.

To find the cycles of a given task, the IMU sensor outputs are used to determine the joint angle signal, which is then smoothed using a Savitzky-Golay smoothing filter. Next, the start and end times of the cycles are established by finding the signal's inflection points. These start and stop times are used to segment the audio data into a matrix of "cycles". For each cycle, the data is further smoothed to ensure the angle is either monotonically increasing or decreasing. Without this step, interpolation of non-monotonically increasing or decreasing data from audio-vs-time to audio-vs-angle signals will result in errors since the algorithm will have more than one audio value for a given angle. By segmenting the data by cycle, we eliminate errors in cycle-to-cycle signal comparison that stem from variations in timing (e.g. slower vs faster exercises). Once the data is segmented, the matrix is restructured using interpolation to define a matrix of audio vs angle signals.

3.5 Wearable System

The wearable system, shown in Figure 4, comprised of a microcontroller (MCU), which collected data from two microphones and inertial measurement units (IMU). A block diagram of the system is provided in Figure 5. The microphone pre-amplifier circuits, MCU, battery (3.7V, 850 mAh Lithium-ion), peripheral components (e.g., switches and LEDs), and one IMU were packaged into the primary box while the second IMU was packaged in its own box. These boxes, which were lightweight aluminum for shielding and comfort purposes, were placed on the lateral side of the thigh and shank respectively.

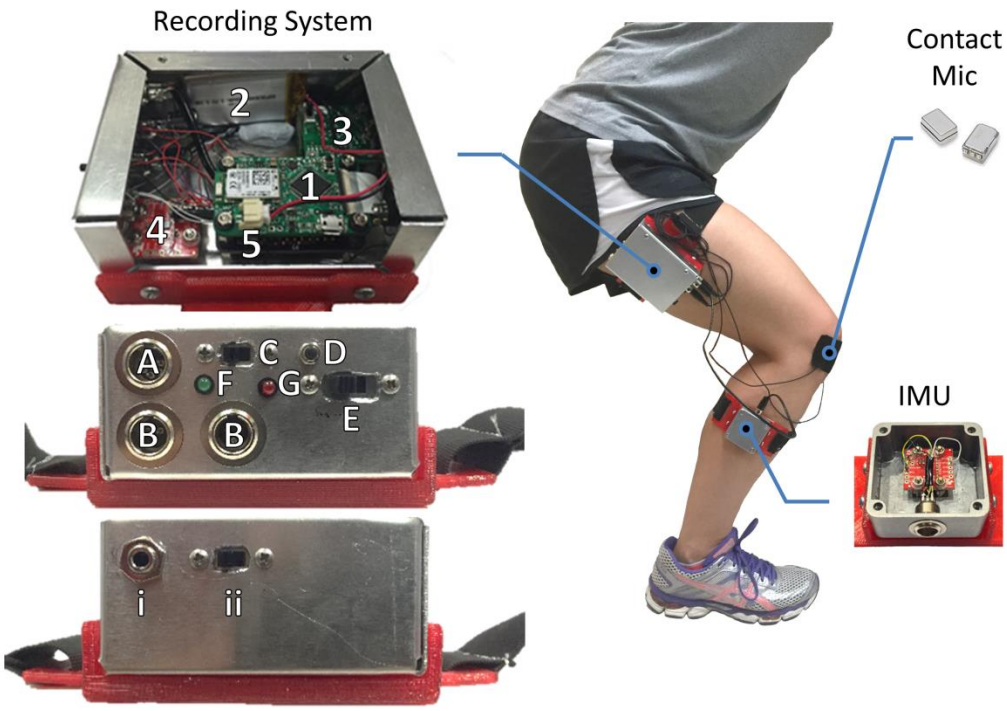

Figure 4. Wearable system for recording joint sounds. The system consists of two enclosures, the primary and secondary enclosure, which house the recording system and shank inertial measurement unit (IMU), respectively. The recording system is comprised of the microcontroller (MCU, labeled 1), battery (2), microphone pre-amplifier circuits (3), thigh IMU (4), and microSD card (5). The primary box panel contains connectors for the shank IMU (A) and microphones (B). Additionally, the front panel of this box has a record slide switch (C), standby mode pushbutton (D), bypass MCU switch (E), and LED indicators for active recording (F) and error notifications (G). Lastly, for engineering use, the back panel contains a microphone selector switch (i) to determine which microphone is outputted to the audio jack (ii).

The wearable system consists of two IMUs and two microphones. The IMUs (LSM6DS3, ST Microelectronics, Geneva, Switzerland) are placed on the lateral sides of the thigh and shank such that joint angle may be extracted using information from the 3-axis accelerometers and 3-axis gyroscopes. The system is compatible with two types of microphones: a piezoelectric-based contact microphone (BU-23173, Knowles, Itasca, IL) to measure acoustic emissions that materialize as vibrations on the skin and a

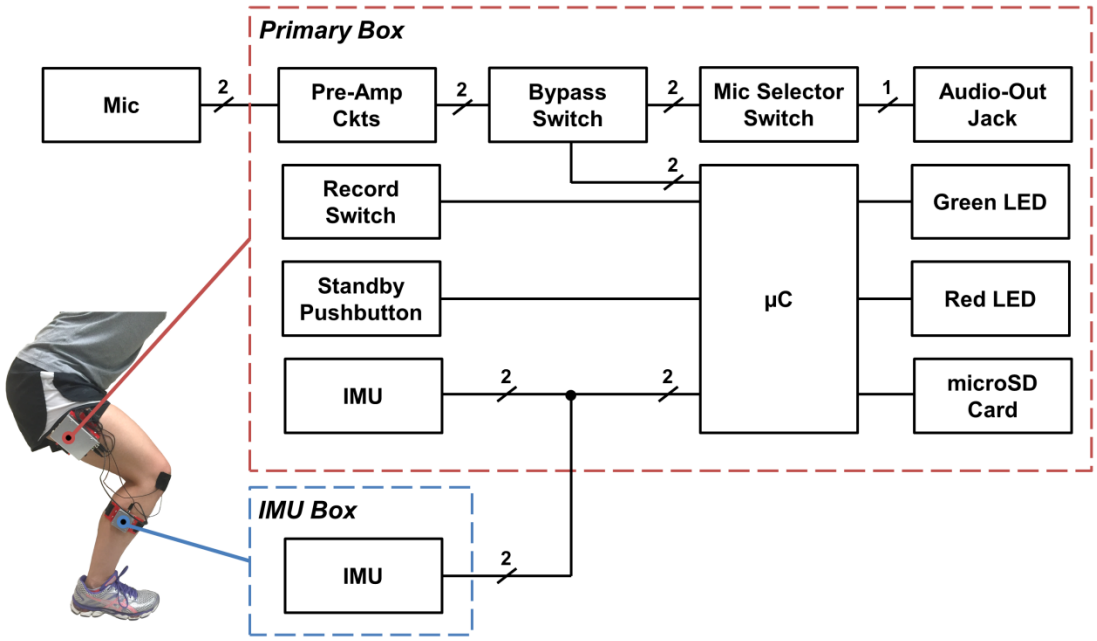

Figure 5. Block diagram of the wearable system. The primary box houses the microphone front-end circuits (x2), an IMU, the microcontroller, and various user peripherals (e.g., pushbuttons, slide switches, and LEDs. The second box contains the IMU placed on the shank.

microelectromechanical systems (MEMS) based microphone (MP33AB01H, ST Microelectronics, Geneva, Switzerland) to measure airborne sounds. At any given time, two microphones, placed at the lateral and medial sides of the patella, may be used to measure acoustic emissions. This work specifically uses the contact microphones to demonstrate functionality of the system.

J. L. Conant designed custom circuits to interface these microphones. The microphone pre-amplifier circuit consists of a non-inverting, adjustable front-end gain stage with a 53 Hz high pass cutoff; a slide switch sets the gain at either 20 or 40 dB depending on type of microphone—contact or MEMS—used. This stage was followed by a sixth-order, Sallen-Key low pass filter with a cutoff frequency of 20 kHz to help reduce

high frequency noise and aliasing. This circuit was powered with a regulated 3V power supply.

The system also included other peripheral components, such as switches and LEDs, for convenience. Buttons and switches include a pushbutton to enter the low-power standby mode, a slide switch to start and stop recording, and a switch to bypass the microcontroller and output one of the microphone signals—selected via the microphone selector switch—to a headphone audio jack. The functions of these components are described in section 3.6, "Embedded System Design". The locations of these switches are shown in Figure 4.

3.6 Embedded System Design

The embedded system used to record data in the wearable system comprised of an ARM® Cortex®-M4-microcontroller (STMF405, STMicroelectronics, Geneva, Switzerland). We used the ChibiOS real-time operating system (RTOS) and hardware abstraction layer (HAL) for development. The system operates in three modes as summarized in Figure 6: 1) standby, 2) awake, and 3) recording. During standby mode, the system is put in a low-power mode and functionality is disabled. When the standby pushbutton is pressed, the MCU activates, entering the awake mode. In this mode, the MCU waits for the user to either begin a recording using the record slide switch or put the system back into standby mode. If the user starts a recording, the MCU will sample two microphone channels at 48 kHz and two IMU devices (3-axis accelerometer and gyroscope data) at 208 Hz and periodically save the data to a microSD card in three separate files: one *.wav file containing the two channels of microphone data and two *.csv files—one for each IMU—containing the six channel IMU data. The various LED on / off / blink configurations are summarized in Table 1.

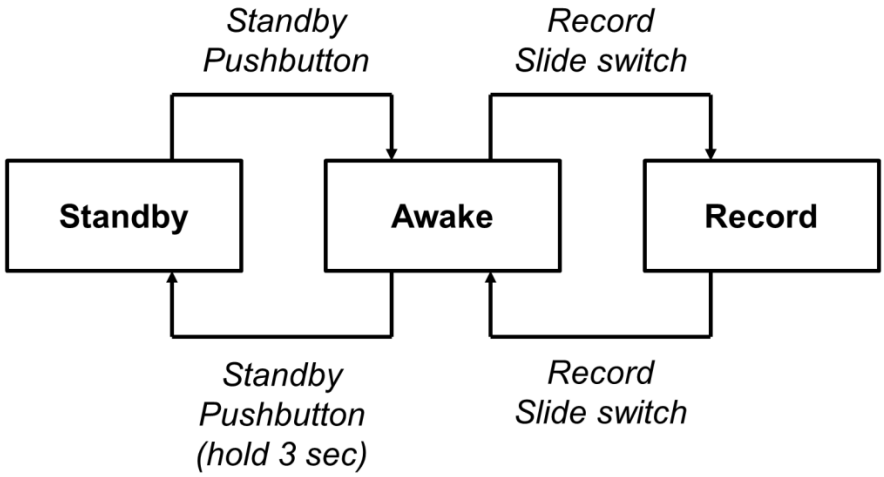

Figure 6. Embedded system state transitions. The system enters the awake state from the standby state via pressing the standby pushbutton. Recording is initiated and stopped using the record slide switch. The system returns to the standby mode by pressing the standby pushbutton for three seconds and cannot be reached directly from the record state.

3.6.1 Standby Mode

To save power when uninterested in recording data, the user can put the MCU into standby mode, which provides the minimum power consumption for this device. In this mode, the static random-access memory (SRAM) and register values are not retained, essentially acting as a hardware reset for the device. Since we do not need to save the contents of various register and memory values between sessions, this does not present as a problem. To enter standby mode, the user must press the pushbutton continuously for three seconds. This option is not available while the device is actively recording data, forcing the user to safely stop recording so that any open files on the microSD card can be closed correctly and consequently free any unused pre-allocated memory. To indicate that the device has entered standby mode, the green LED will turn off (the red LED will

Table 1. LED Configurations for Wearable System

LED Configuration	Current State	Meaning
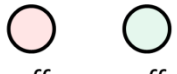	Standby	Device is in low-power mode
	Awake	Device waiting for user action
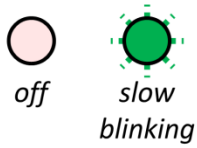	Record	Begin recording
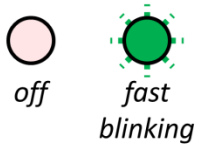	Record	Successful recording
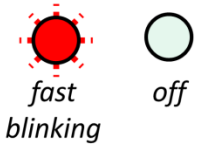	Record	Error encountered

have been previously been off). The user can activate the system and exit standby mode (i.e., enter the awake mode) by pressing the pushbutton again.

3.6.2 Awake Mode

Once the device enters the awake state, the green LED will turn on. In this mode, the device waits for the pushbutton to be pressed, entering standby mode, or the record slide switch to change to the record position, starting a data collection session, which is indicated by a slowly blinking green LED.

3.6.3 Record Mode

We utilize the file allocation table (FAT) file system (FatFs) (ChaN, 2016) to manage and write our data files to the microSD card. Any microSD cards used must be formatted to use this file system. When a recording session starts, we first pre-allocate memory for each of the data files on the microSD card. By pre-allocating memory, we do not have to update the file size on disk with each write, which saves us crucial time since we continuously and frequently write to the microSD card. We chose to pre-allocate approximately 8.5 minutes' worth of memory, which is satisfactory for our application given that we analyze five repeated exercises that usually last less than a minute.

In addition to setting up the files before actual samples are taken, we initialize the hardware. First, the 12-bit analog-to-digital converter (ADC) is initialized to sample two channels—one for each microphone—at 48 kHz. To accommodate this high sample rate, the ADC is configured to automatically save the samples into a circular buffer. This buffer is sized to be a multiple of 512 bytes in length because the microSD card performs the fastest writes when writing large blocks of sector-sized data chunks (512 bytes/sector).

Second, the IMUs are initialized to run in normal-mode at 208 Hz with interrupt generation to act as a data-ready line. Similar to the ADC, the IMU samples are stored in N·512-byte circular buffers to improve microSD write speed. To communicate with the IMUs, we use I^2C with a clock line of 150 kHz and slow pin-change speed. These settings were selected to reduce the amount of noise on the ADC lines while maintaining sufficient bus throughput.

Once the hardware and files on the microSD card are initialized, the MCU begins sampling data. When half of a buffer is full for the ADC or one of the IMUs, the MCU goes to write the half-buffer worth of data to the microSD card. The IMUs are synched with the microphone data by writing the current microphone sample number to the *.csv files. Occasionally due to timing or a random slow-write, the microSD card will not be done writing data when a new buffer-ready signal is generated, otherwise known as an overrun. When an overrun occurs, the next data cannot be trusted to be correct, so placeholder zero values are written to the microSD card such that all sensors remain sample-synched. Generally, multiple overruns will occur sequentially while the microSD card tries to "catch-up" with the incoming sample data, but typically these will account for less than 0.5 seconds of data.

Once the user has completed the exercise, he can trigger the MCU to stop recording by moving the slide switch back to its original position. When the MCU recognizes this, it will stop sampling, flush any data that was buffered but not written to the microSD card, and close all files. To indicate a successful recording, the green LED will quickly blink for five seconds before returning to the on state. If the MCU encountered an error at any point during the code (e.g. no microSD card in place, improper initialization of IMUs, error writing the microSD card entirely, too many overruns for the recording to be useful, etc.), the MCU will safely stop the record sequence and quickly blink the red LED for 5 seconds.

CHAPTER 4. RESULTS

4.1 Measuring Joint Sounds during Unloaded Knee Flexion / Extension

Example signals obtained from one subject are shown in Figure 7. These sounds were obtained using the MEMS microphones placed at the lateral side of the patella. The subject had an ACL and meniscus tear many years prior to the study (both on the right side, and both repaired via reconstructive surgery), while the left knee is injury-free. Interestingly, we noticed that the number of high frequency signature markers that represent a "click" (i.e., acoustic emissions) were more notable on the right side compared to the left. For both knees, we observed that the microphone signal shape was consistent from one cycle to the next, with the main acoustic emissions occurring at the same location within the cycle based on the IMU measures.

4.2 Measuring Joint Sounds during a Multi-Joint, Weight-Bearing Movement (Sit-to-Stand)

Example signals from a different subject performing sit-to-stand exercises are shown in Figure 8. These sounds were obtained with the COS-11D microphones placed at the lateral side of the patella. In this figure, to observe the consistency of the sounds as a function of joint angle, we have plotted each of the sit-to-stand cycles on the same axes, with an artificial offset such that the timings can be readily compared. The blue traces show the sounds as the subject moves from a seated to standing position; the red traces as the subject moves back to the seated position. The sounds were consistent in nature for the five consecutive repetitions of the sit-to-stand activity both in terms of morphology of

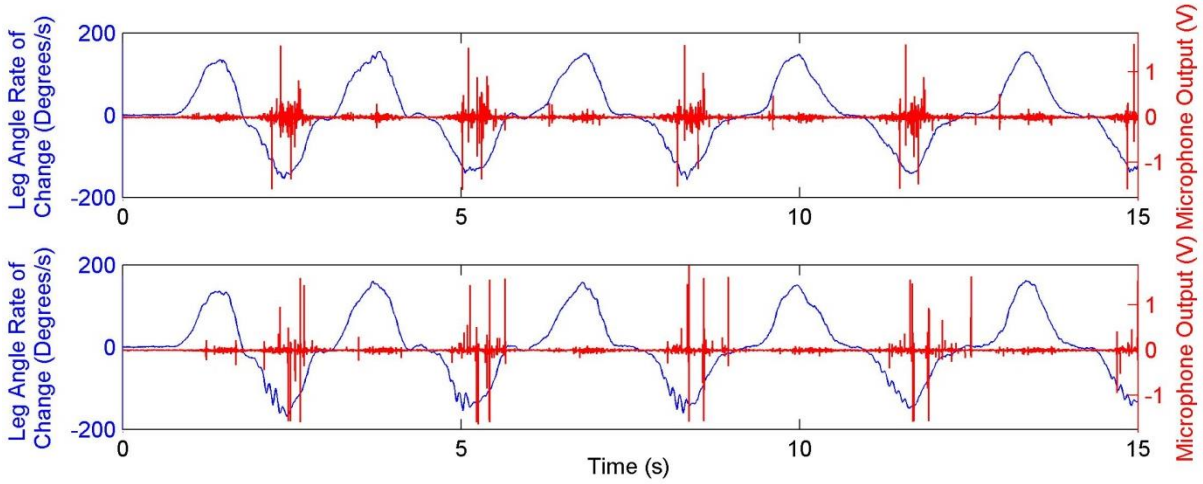

Figure 7. Joint sounds and associated IMU data (angle rate of change) for the left (top) and right (bottom) knees of a subject without acute injury for four consecutive flexion / extension cycles. The joint sounds are very consistent from one flexion / extension cycle to the next, for both knees. The subject had an anterior collateral ligament (ACL) and meniscus tear many years prior to the recordings (both on the right side, and both repaired via surgery), while the left knee is injury-free. Interestingly, we found more frequent, high frequency "clicks" on the right side compared to the left, a feature of the sounds that we will study further in future work.

each of the acoustic emissions, and the timing of the emissions with respect to joint angle.

4.3 Comparison of Piezoelectric Contact and Electret Microphones for Joint Sounds

Figure 9 shows a series of flexion and extension cycles performed with both the electret (COS-11D) and contact microphones placed on the knee joint and measured simultaneously. The top portion of the figure shows the time traces of the electret and contact microphone signals. High frequency joint sounds are captured simultaneously by both sensing modalities, which support the theoretical expectation: while joint sounds that materialize as skin vibrations will be broadband in nature (i.e., containing both low

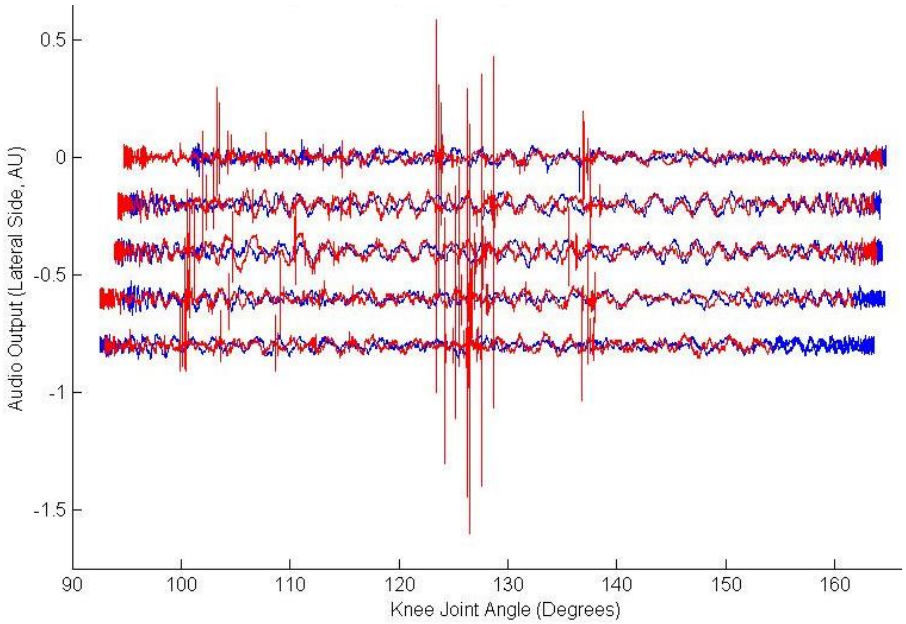

Figure 8. Joint sounds plotted against knee joint angle for five consecutive sit-to-stand tests. The blue traces show the sounds as the subject moves from a seated to standing position; the red traces show the subject moving from the standing position back to the seated position. The consistency in the sounds was striking in terms of where the high frequency emissions occurred with respect to joint angle.

and high frequency signals), airborne joint sounds will only contain the higher frequency content.

A spectrogram based depiction of the frequency content of the sounds as a function of time is also provided on the bottom of Figure 9. The piezoelectric microphone in contact with the skin clearly provided a higher ratio of signal power to background noise, as evident in both the time and frequency domain. Additionally, the main acoustic emission event during the flexion cycle was concurrent on both types of microphone recordings; however, overall, the piezoelectric contact microphone provided more details and, in particular, more frequency content in the lower end of the range (1 kHz – 5 kHz). These recordings support the theoretical expectation that in the ideal scenario, when the microphones are affixed to the skin using tape and thus cannot move away from the skin

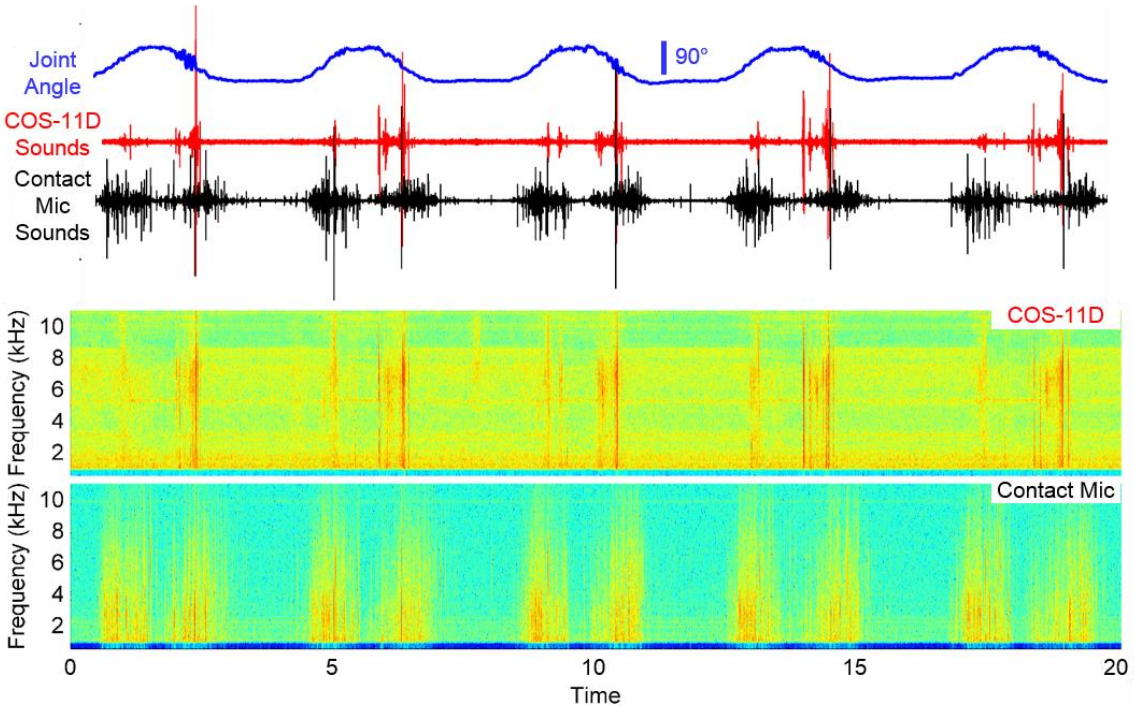

Figure 9. Joint sounds simultaneously acquired by a COS-11D electret microphone and a piezoelectric contact microphone in the time domain (top) and via short-time Fourier transform (STFT) based time-frequency visualization (bottom). The background noise level was much lower for the contact microphones, due to their direct pick-up of skin vibration as compared to airborne sounds. The higher frequency (> 5 kHz) components were more pronounced for the electret microphones, while the lower frequency components (< 5 kHz) were more pronounced for the contact microphones. The cyclic signatures of both types of microphones for each flexion / extension cycle were consistent.

surface, the piezoelectric contact microphone provides a better signal as compared to the electret microphone.

4.4 Measurement of Airborne Sounds 5 cm Off of the Skin

Figure 10 shows the joint sounds for one subject measured with the COS-11D microphones placed directly on the skin (top set of traces), and placed 5 cm off of the skin (bottom set of traces). Although the signal level was lower (by 4x) for the joint sound signals taken away from the skin compared to directly on the skin, similar

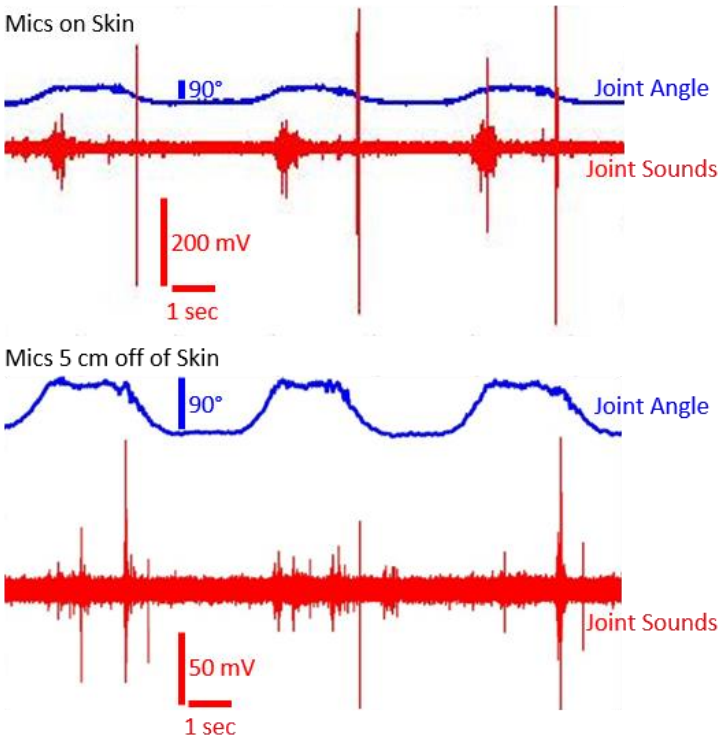

Figure 10. Joint sounds measured together with joint angle for a subject performing flexion / extension repetitions. The top set of traces shows the signals when the mics are placed directly on the skin, while the bottom set shows the signals with the mics positioned in the air, 5 cm off of the skin surface. While positioning the mics off of the skin decreased the signal level, the main acoustic emission peaks occurred at similar instants within the flexion and extension cycles, demonstrating that even in the absence of direct contact, sounds can be measured with these miniature microphones.

signatures were obtained – for example, the largest peak occurring in the middle of the flexion cycle was apparent in both sets of measurements, as was the large peak occurring at maximal extension. This demonstrates that the electret microphones, which sense airborne sounds, can still measure the acoustic emissions from the joint even in the absence of direct contact to the skin (for example, if the user moves and the microphone detaches from the skin surface).

4.5 Embedded System

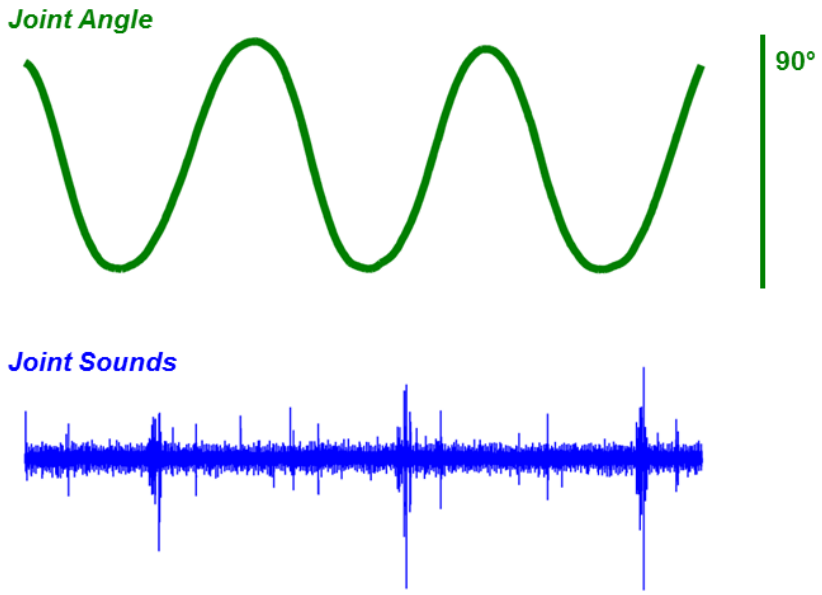

Figure 11. An example measurement of joint sounds, recorded from the lateral side of the patella, in the context of knee joint angle, which was extracted from two IMUs placed at the lateral side of the thigh and shank. The sounds were recorded during an unloaded flexion / extension task.

Table 2. Current Consumption of Wearable Device*

Operating Mode	Supply Current (mA)
standby	5
awake	44
recording (nominal)	62
recording (max)	110

*The system is powered off a 3.7V, 850mAh Lithium-ion battery, which is then regulated down to 3V.

Using this low-power wearable system, we were able to successfully record simultaneous joint acoustic emissions and IMU data. An example successful recording is shown in Figure 11. Note that joint angle can be extracted from successful recordings of IMU data via various algorithms (e.g., [10]). This system provides a more practical, low-power alternative to our previous wearable systems (see Table 2) [11]. However, there exist various limitations and areas of improvement for future iterations in terms of noise,

robustness, and power consumption. For example, while we implemented methods, such as decreasing the I^2C pin-change speed and limiting the clock speed to 150 kHz, to reduce noise on the ADC pins due to digital communication, using an external ADC would further reduce the noise of the analog microphone channels. In terms of robustness, because the MCU looks for a single rising edge to exit standby mode, any accidental pressing of the pushbutton or switch bounces will wake the MCU. This current version of the system relies on the user to recognize such errors via the green LED and put the MCU back into standby mode; however, future iterations may employ a slide switch, switch debouncing hardware techniques, or use a timeout that puts the system to sleep if left untouched for a few minutes to mitigate this issue. It should be noted that during standby mode only the MCU is put into a low-power mode. The microphone front-end circuits and various peripherals such as the microSD circuit and portions of the IMU hardware modules remain active. To reduce the power consumption further, smart power management may be investigated.

CHAPTER 5. DISCUSSION

This thesis presents preliminary findings from joint sound measurements at the knee in the context of specific activities (e.g. unloaded flexion / extension and sit-to-stand). An important observation was that the morphology and timing of the joint sounds was consistent for several repetitions of the same activity, and the main acoustic emissions occurred at consistent joint angles. However, this work does not present these findings quantitatively; future work shall consider metrics for quantifying the consistency of significant acoustic emissions. While consistent acoustic emissions as a feature, or biomarker, may not present to be physiologically-relevant (e.g., characteristic of healthy knees versus those with ACL tears), it does show that the hardware can sufficiently measure the sounds consistently, which is important considering the ultimate objective of measuring sounds in an unsupervised setting.

Additionally, the sounds obtained from an electret microphone placed on the skin and one located 5 cm off the skin captured similar acoustic signals in both morphology and timing. This is an important observation because it suggests that the air microphones will be able to record joint sounds in a wearable device where direct contact with the skin may not be constant. However, it will be important to consider this distance when analyzing the captured signals, particularly when the analysis depends on the amplitude of the signal. In this sense, maintaining a fixed distance between the microphone and skin, especially for use in longitudinal analysis, will be required. Furthermore, placing the microphone off of the skin introduces increased potential for noise; the microphone may have a greater opportunity to strike or rub against the skin. Additionally, changing the

distance between the microphone and skin will change the microphone's sensitivity in sensing these sounds. These issues must be addressed in the design of a wearable system.

The preliminary wearable system provides a more practical, low-power alternative to our in-lab / in-clinic systems. However, there exist various limitations and areas of improvement for future iterations in terms of noise, robustness, and power consumption. For example, while we implemented methods, such as decreasing the I^2C pin-change speed and limiting the clock speed to 150 kHz, to reduce noise on the ADC pins due to digital communication, using an external ADC would further reduce the noise of the analog microphone channels. In terms of robustness, because the MCU looks for a single rising edge to exit standby mode, any accidental pressing of the pushbutton or switch bounces will wake the MCU. Moreover, this current version of the wearable system relies on the user to recognize such errors via the green LED and put the MCU back into standby mode; however, future iterations may employ a slide switch, switch debouncing hardware techniques, or use a timeout that puts the system to sleep if left untouched for a few minutes to mitigate this issue. It should be noted that during standby mode only the MCU is put into a low-power mode. The microphone front-end circuits and various peripherals such as the microSD circuit and portions of the IMU hardware modules remain active. To reduce the power consumption further, smart power management may be investigated. Lastly, this iteration of the wearable system focused solely on the recording instrumentation. Future iterations will need to consider the packaging of microphones around the knee without the use of tape, for wearability, namely unobtrusiveness, of the system is important so as not to dissuade users from wearing the device longitudinally.

CHAPTER 6. CONCLUSION

Preliminary work towards a wearable joint rehabilitation device was completed. Two areas of work were completed: (1) determining the efficacy of measuring knee joint sounds using air and contact microphones and (2) implementing an initial wearable data acquisition system. During the first phase, various types of microphones for sensing joint sounds were selected; electret and MEMS-based microphones were chosen for sensing airborne sounds, while a piezoelectric film sensor was selected for sensing sounds that materialize as skin surface vibrations. Using these microphones and custom front-end circuits, various proof-of-concept experiments were completed for in-lab settings. Three significant conclusions were reached: (1) significant acoustic emissions occurred at consistent angles for repeated exercises, (2) significant, high frequency acoustic emissions were measured simultaneously on all three types of microphones, and (3) air microphones were capable of capturing joint sounds both directly on the skin and 5 cm off the skin (i.e., did not require direct proximity to sense joint sounds).

Given the ultimate objective of a wearable system, the second phase of this work focused on development of an initial wearable embedded-system-based prototype for measuring joint sounds. We implemented microcontroller RTOS-based software with sufficiently high sampling rate capabilities (48 kHz) to obtain joint sounds and save the data to a microSD card. Simultaneously, 6-axis inertial data from two sensors were sampled and saved as well.

Using these or similar sensing systems, future work shall focus on investigating features of acoustic emissions from the knee to provide information about the

physiological state of the joint itself. Namely, research shall explore the possibility of providing a return-to-play metric based on acoustic emissions, thus presenting a quantitative alternative that is directly related to the joint rather than rely on its derivatives (e.g., surrounding muscle strength, results of single-leg hop tests, and patient-described self-confidence in performing cutting and pivoting motions). Moreover, features of acoustic emissions may be able to provide estimates on when a patient may move forward in his rehabilitation; for instance, possible features may indicate when a patient may begin weight-bearing running exercises. Importantly, using acoustic emissions for joint health analysis is novel compared to current clinical practices (e.g., various imaging techniques such as MRI scans) in that it provides quantitative data during dynamic motions. In this sense, the biomechanical function of joint can be analyzed, which is not currently available from most commonly used imaging techniques. For such objectives, robust measurements of joint sounds are required; this work aimed to validate possible sensing capabilities for measuring joint sounds in a wearable form factor.

REFERENCES

[1] O. T. Hill, A. B. Kay, M. M. Wahi, C. J. McKinnon, L. Bulathsinhala, and T. F. Haley, “Rates of knee injury in the U.S. Active Duty Army, 2000-2005,” *Mil Med,* vol. 177, no. 7, pp. 840-4, Jul, 2012.

[2] T. D. Lauder, S. P. Baker, G. S. Smith, and A. E. Lincoln, "Sports and physical training injury hospitalizations in the army," *Am J Prev Med*, 3 Suppl, pp. 118-28, Netherlands, 2000.

[3] P. Bonato, "Advances in wearable technology and applications in physical medicine and rehabilitation," *J of NeuroEngineering and Rehabilitation*, 2005, pp. 1-4.

[4] O. Unluhisarcikli, M. Pietrusinski, B. Weinberg, P. Bonato, and C. Mavroidis "Design and control of a robotic lower extremity exoskeleton for gait rehabilitation," *Intelligent Robots and Systems (IROS), 2011 IEEE/RSJ International Conference on, 2011,* pp. 4893-4898.

[5] K.-H. Chen, P.-C. Chen, K.-C. Liu, and C.-T. Chan, “Wearable sensor-based rehabilitation exercise assessment for knee osteoarthritis,” *Sensors*, vol. 15, no. 2, pp. 4193, 2015.

[6] C. Glaros, D. I. Fotiadis, A. Likas, and A. Stafylopatis, "A wearable intelligent system for monitoring health condition and rehabilitation of running athletes," *Proc of the 4th Annual IEEE Conf on Information Technology Applications*, pp. 276-279.

[7] L. Atallah, G. G. Jones, R. Ali, J. J. H. Leong, B. Lo, and Y. Guang-Zhong, "Observing Recovery from Knee-Replacement Surgery by Using Wearable Sensors," *Body Sensor Networks (BSN), 2011 International Conference on, Dallas, TX*, pp. 29-34, Dallas, TX, 2011.

[8] S. Shrivastava, and R. Prakash, "Assessment of bone condition by acoustic emission technique: A review," *J. Biomedical Science and Engineering*, 2009, vol. 2, pp. 144-154.

[9] C. B. Frank, R. M. Rangayyan, and G. D. Bell, “Analysis of knee joint sound signals for non-invasive diagnosis of cartilage pathology,” *IEEE Engineering in Medicine and Biology Magazine,* vol. 9, no. 1, pp. 65-68, 1990.

[10] D. Glaser, R. D. Komistek, H. E. Cates, and M. R. Mahfouz, “A non-invasive acoustic and vibration analysis technique for evaluation of hip joint conditions,” *Journal of Biomechanics,* vol. 43, no. 3, pp. 426-432.

[11] K. S. Kim, J. H. Seo, and C. G. Song, “An acoustical evaluation of knee sound for non-invasive screening and early detection of articular pathology,” *Journal of Medical Systems,* vol. 36, no. 2, pp. 715-722, 2012.

[12] B. Mascaro, J. Prior, L. K. Shark, J. Selfe, P. Cole, and J. Goodacre, “Exploratory study of a non-invasive method based on acoustic emission for assessing the dynamic integrity of knee joints,” *Med. Eng. Phys.,* vol. 31, no. 8, pp. 1013-22, Oct, 2009.

[13] C. Teague, S. Hersek, H. Töreyin, M. L. Millard-Stafford, M. L. Jones, G. F. Kogler, M. N. Sawka, and O. T. Inan, "Novel approaches to measure acoustic emissions as biomarkers for joint health assessment," *Body Sensor Networks (BSN), 2015 International Conference on, Cambridge, MA*, Cambridge, MA, 2015.

[14] C. Teague, N., S. Hersek, J. L. Conant, S. M. Gilliland, and O. T. Inan, "Wearable knee health rehabilitation assessment using acoustical emissions," *Review of Progress in Quantitative Nondestructive Evaluation,* 2016.

[15] “Anterior Cruciate Ligament Injury: SurgicalConsiderations,” *American Academy of Orthopaedic Surgeons,* 2007.

[16] S. D. Barber-Westin, and F. R. Noyes, “Factors used to determine return to unrestricted sports activities after anterior cruciate ligament reconstruction,” *Arthroscopy,* vol. 27, no. 12, pp. 1697-705, Dec, 2011.

[17] P. D. Austermuehle, “Common knee injuries in primary care,” *Nurse Practitioner,* vol. 26, no. 10, pp. 26, 2001.

[18] B. E. Gage, N. M. McIlvain, C. L. Collins, S. K. Fields, and R. D. Comstock, “Epidemiology of 6.6 million knee injuries presenting to United States emergency departments from 1999 through 2008,” *Acad. Emerg. Med.,* vol. 19, no. 4, pp. 378-85, Apr, 2012.

[19] P. J. McMahon, and H. B. Skinner, "Sports medicine," *Current diagnosis & treatment in orthopedics,* H. B. Skinner, ed., pp. 155-173, New York: Lange Medical Books, 2003.

[20] W. C. Whiting, "Biomechanics of musculoskeletal injury," R. F. Zernicke, ed., Champaign, IL, 2008, pp. 166-184.

[21] C. R. Allen, G. A. Livesay, E. K. Wong, and S. L. Woo, “Injury and reconstruction of the anterior cruciate ligament and knee osteoarthritis,” *Osteoarthritis Cartilage,* vol. 7, no. 1, pp. 110-21, Jan, 1999.

[22] S. M. Gianotti, S. W. Marshall, P. A. Hume, and L. Bunt, “Incidence of anterior cruciate ligament injury and other knee ligament injuries: a national population-based study,” *J Sci Med Sport,* vol. 12, no. 6, pp. 622-7, Nov, 2009.

[23] E. Alentorn-Geli, G. D. Myer, H. J. Silvers, G. Samitier, D. Romero, C. Lazaro-Haro, and R. Cugat, "Prevention of non-contact anterior cruciate ligament injuries in soccer players. Part 1: Mechanisms of injury and underlying risk factors," *Knee Surg Sports Traumatol Arthrosc,* vol. 17, no. 7, pp. 705-29, Jul, 2009.

[24] C. L. Ardern, K. E. Webster, N. F. Taylor, and J. A. Feller, "Return to the preinjury level of competitive sport after anterior cruciate ligament reconstruction surgery: two-thirds of patients have not returned by 12 months after surgery," *Am J Sports Med,* vol. 39, no. 3, pp. 538-43, Mar, 2011.

[25] V. M. Shah, J. R. Andrews, G. S. Fleisig, C. S. McMichael, and L. J. Lemak, "Return to play after anterior cruciate ligament reconstruction in National Football League athletes," *Am J Sports Med,* vol. 38, no. 11, pp. 2233-9, Nov, 2010.

[26] R. H. Brophy, L. Schmitz, R. W. Wright, W. R. Dunn, R. D. Parker, J. T. Andrish, E. C. McCarty, and K. P. Spindler, "Return to play and future ACL injury risk after ACL reconstruction in soccer athletes from the Multicenter Orthopaedic Outcomes Network (MOON) group," *Am J Sports Med,* vol. 40, no. 11, pp. 2517-22, Nov, 2012.

[27] G. D. Myer, M. V. Paterno, K. R. Ford, C. E. Quatman, and T. E. Hewett, "Rehabilitation after anterior cruciate ligament reconstruction: criteria-based progression through the return-to-sport phase," *J Orthop Sports Phys Ther,* vol. 36, no. 6, pp. 385-402, Jun, 2006.

[28] C. L. Ardern, K. E. Webster, N. F. Taylor, and J. A. Feller, "Return to sport following anterior cruciate ligament reconstruction surgery: a systematic review and meta-analysis of the state of play," *Br J Sports Med,* vol. 45, no. 7, pp. 596-606, Jun, 2011.

[29] T. E. Hewett, S. L. Di Stasi, and G. D. Myer, "Current concepts for injury prevention in athletes after anterior cruciate ligament reconstruction," *Am J Sports Med,* vol. 41, no. 1, pp. 216-24, Jan, 2013.

[30] B. E. Oiestad, L. Engebretsen, K. Storheim, and M. A. Risberg, "Knee osteoarthritis after anterior cruciate ligament injury: a systematic review," *Am J Sports Med,* vol. 37, no. 7, pp. 1434-43, Jul, 2009.

[31] A. M. W. Chaudhari, P. L. Briant, S. L. Bevill, S. Koo, and T. P. Andriachhi, "Knee Kinematics, Cartilage Morphology, and Osteoarthritis after ACL Injury," *Medicine & Science in Sports & Exercise,* vol. 40, no. 2, pp. 215-222, 2008.

[32] L. S. Lohmander, A. Ostenberg, M. Englund, and H. Roos, "High prevalence of knee osteoarthritis, pain, and functional limitations in female soccer players twelve years after anterior cruciate ligament injury," *Arthritis Rheum,* vol. 50, no. 10, pp. 3145-52, Oct, 2004.

[33] M. A. Kessler, H. Behrend, S. Henz, G. Stutz, A. Rukavina, and M. S. Kuster, "Function, osteoarthritis and activity after ACL-rupture: 11 years follow-up results of conservative versus reconstructive treatment," *Knee Surgery, Sports Traumatology, Arthroscopy*, vol. 16, no. 5, pp. 442-448, 2008.

[34] O. Andreykiv, V. Skalsky, O. Serhiyenko, and D. Rudavskyy, "Acoustic emission estimation of crack formation in aluminium alloys," *Engineering Fracture Mechanics*, vol. 77, no. 5, pp. 759-767, 3, 2010.

[35] M. Wevers, "A selection of papers presented at the First Joint Belgian-Hellenic Conference on NDTListening to the sound of materials: Acoustic emission for the analysis of material behaviour," *NDT & E International*, vol. 30, no. 2, pp. 99-106, 1997/04/01, 1997.

[36] O. Stankevych, and V. Skalsky, "Investigation and identification of fracture types of structural materials by means of acoustic emission analysis," *Engineering Fracture Mechanics*, vol. 164, pp. 24-34, 9, 2016.

[37] A. Gurung, C. G. Scrafford, J. M. Tielsch, O. S. Levine, and W. Checkley, "Computerized lung sound analysis as diagnostic aid for the detection of abnormal lung sounds: A systematic review and meta-analysis," *Respiratory Medicine*, vol. 105, no. 9, pp. 1396-1403, 9, 2011.

[38] A. Kandaswamy, C. S. Kumar, R. P. Ramanathan, S. Jayaraman, and N. Malmurugan, "Neural classification of lung sounds using wavelet coefficients," *Computers in Biology and Medicine*, vol. 34, no. 6, pp. 523-537, 9//, 2004.

[39] S. Babaei, and A. Geranmayeh, "Heart sound reproduction based on neural network classification of cardiac valve disorders using wavelet transforms of PCG signals," *Computers in Biology and Medicine*, vol. 39, no. 1, pp. 8-15, 1//, 2009.

[40] S. C. Abbott, and M. D. Cole, "Vibration arthrometry: a critical review," *Crit. Rev. Biomed. Eng.*, vol. 41, no. 3, pp. 223-42, 2013.

[41] J. H. Lee, C. C. Jiang, and T. T. Yuan, "Vibration arthrometry in patients with knee joint disorders," *IEEE Trans. Biomed. Eng.*, vol. 47, no. 8, pp. 1131-3, Aug, 2000.

[42] R. A. Mollan, G. C. McCullagh, and R. I. Wilson, "A critical appraisal of auscultation of human joints," *Clin Orthop Relat Res*, no. 170, pp. 231-7, Oct, 1982.

[43] L. K. Shark, H. Chen, and J. Goodacre, "Discovering differences in acoustic emission between healthy and osteoarthritic knees using a four-phase model of sit-stand-sit movements," *Open Med. Inform. J.*, vol. 4, pp. 116-25, 2010.

[44] Y. Wu, S. Krishnan, and R. M. Rangayyan, "Computer-aided diagnosis of knee-joint disorders via vibroarthrographic signal analysis: a review," *Crit. Rev. Biomed. Eng.*, vol. 38, no. 2, pp. 201-24, 2010.